Published in final edited form as:

J Comp Neurol. 2020 July ; 528(10): 1660–1671. doi:10.1002/cne.24850.

Expression and distribution of Trophoblast Glycoprotein in the mouse retina

Colin M Wakeham[1], **Gaoying Ren**[1], **Catherine W Morgans**[1]

[1]Department of Chemical Physiology & Biochemistry, Oregon Health & Science University, Portland, OR 97239, USA

Abstract

We recently identified the leucine-rich repeat (LRR) adhesion protein, trophoblast glycoprotein (TPBG), as a novel PKCα-dependent phosphoprotein in retinal rod bipolar cells (RBCs). Since TPBG has not been thoroughly examined in the retina, this study characterizes the localization and expression patterns of TPBG in the developing and adult mouse retina using two antibodies, one against the N-terminal LRR domain and the other against the C-terminal PDZ-interacting motif. Both antibodies labeled RBC dendrites in the OPL and axon terminals in the IPL, as well as a putative amacrine cell with their cell bodies in the inner nuclear layer (INL) and a dense layer in the middle of the inner plexiform layer (IPL). In live transfected HEK293 cells, TPBG was localized to the plasma membrane with the N-terminal LRR domain facing the extracellular space. TPBG immunofluorescence in RBCs was strongly altered by the loss of TRPM1 in the adult retina, with significantly less dendritic and axon terminal labeling in TRPM1 knockout compared to wild type, despite no change in total TPBG detected by immunoblotting. During retinal development, TPBG expression increases dramatically just prior to eye opening with a time course closely correlated with that of TRPM1 expression. In the retina, LRR proteins have been implicated in the development and maintenance of functional bipolar cell synapses, and TPBG may play a similar role in RBCs.

Graphical Abstract

TPBG is a leucine-rich repeat glycoprotein with an intracellular PDZ-binding motif that is localized to the dendrites and axon terminals of retinal rod bipolar cells and in the cell body and dendrites of an uncharacterized amacrine cell. Immunofluorescent labeling of TPBG in rod bipolar cells is significantly reduced in the TRPM1 knockout retina, yet total retinal TPBG is constant. This suggests that antibody access may be blocked in certain activity states, possibly by TPBG binding to a PDZ protein in a light- or phosphorylation-dependent manner.

Corresponding author: Catherine W Morgans, Chemical Physiology & Biochemistry, L-334, Oregon Health & Science University, 3181 SW Sam Jackson Park Rd, Portland, OR 97239, morgansc@ohsu.edu.

Author contributions: study design: CMW, CWM; experimentation: CMW, GR; figure and manuscript preparation: CMW, CWM; editing and review: CMW, GR, CWM

Data availability statement: The data that support the findings of this study are available from the corresponding author upon reasonable request.

Conflict of interest statement: The authors declare no conflicts of interest.

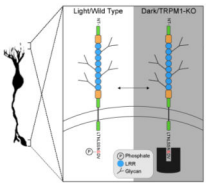

Keywords

retina; synapse; rod bipolar cell; amacrine cell; leucine-rich repeat protein; trophoblast glycoprotein; development; RRID AB_11144484; RRID AB_2801549; RRID AB_2272148; RRID AB_477375; RRID AB_2069567; RRID AB_399431; RRID AB_10846469; RRID AB_2242334; RRID AB_2338052; RRID AB_2340745; RRID AB_2338680; RRID 2721181; RRID AB_2650427; RRID AB_2716622; RRID CVCL_0045

1. Introduction

Rod bipolar cells (RBCs) are the first excitatory interneurons in the primary rod pathway. They receive light-dependent synaptic input from rod photoreceptors in the outer plexiform layer (OPL) and contribute to retinal output via AII amacrine cells in the inner plexiform layer (IPL). RBCs have mostly been studied in the context of dark-adapted, low-light vision (Euler, Haverkamp, Schubert, & Baden, 2014), yet evidence suggests that RBCs contribute to retinal output under a diverse range of lighting conditions. Under completely dark-adapted conditions, RBCs are sensitive to single-photon responses in rods (Berntson, Smith, & Taylor, 2004; Sampath & Rieke, 2004), while under mesopic conditions, RBCs contribute to the perception of contrast (Abd-El-Barr et al., 2009; Ke et al., 2014). In bright light, RBCs may modulate the cone pathway when rods are saturated (Szikra et al., 2014). The molecular mechanisms required for RBC adaptation to changing luminance conditions are mostly unknown, but compelling evidence implicates the commonly-used RBC marker protein kinase C-alpha (PKCα; (Rampino & Nawy, 2011; Ruether et al., 2010; Wakeham et al., 2019; Xiong et al., 2015).

To gain insight into the mechanisms by which PKCα modulates the RBC light response, we sought to identify RBC proteins that undergo PKCα-dependent phosphorylation. Using a multiplexed tandem mass tag mass spectroscopy-based approach, we previously identified trophoblast glycoprotein (TPBG, also known as 5T4 or WAIF1 [Wnt-activated inhibitory factor 1]) as a novel PKCα-dependent phosphoprotein in RBCs (Wakeham et al., 2019). TPBG is a type 1 transmembrane glycoprotein with an N-terminal extracellular domain composed of eight leucine rich repeats (LRRs) interspersed by seven N-linked glycosylation sites. The intracellular cytoplasmic domain is capped by a class 1 PDZ-interacting motif (Zhao, Malinauskas, Harlos, & Jones, 2014) and contains two serines, which were significantly more likely to be phosphorylated in wild type retinas compared to PKCα knockout (Wakeham et al., 2019).

TPBG was first identified in trophoblasts (Hole & Stern, 1988) and has been mainly studied in embryonic development and in cancer (Barrow, Ward, Rutter, Ali, & Stern, 2005), where it is required for chemokine signaling (McGinn, Marinov, Sawan, & Stern, 2012; Southgate

et al., 2010), and where it is diagnostic for metastasis and poor prognosis in cancer patients (Pukrop & Binder, 2008; Weeraratna et al., 2002). In mammalian embryonic cell lines, TPBG influences cytoskeletal organization and cell motility through modulation of Wnt signaling (Kagermeier-Schenk et al., 2011), and has also been shown to interact with scaffolding protein to regulate cell-surface expression of receptors and transporters (Awan et al., 2002). In adult tissues, it is expressed at high levels in ovary, brain, and retina (Imamura et al., 2006; King, Sheppard, Westwater, Stern, & Myers, 1999). Little is known about the role of TPBG in neurons except in the olfactory bulb, where TPBG has been shown to drive developmental changes in the dendritic morphology of granule cell interneurons in an activity-dependent manner, and genetic knockdown of TPBG resulted in impaired odor discrimination (Takahashi et al., 2016; Yoshihara et al., 2012; Yoshihara, Takahashi, & Tsuboi, 2016).

In the retina, a comprehensive single-cell drop-seq study identified TPBG as a possible new RBC marker and clustered it with proteins involved in lamination and adhesion (Shekhar et al., 2016). In a subsequent comparative meta-analysis of RBC transcriptomics studies, it was grouped as a protein potentially implicated in synapse assembly (Woods, Mountjoy, Muir, Ross, & Atan, 2018). TPBG's diverse functions in other tissues suggest potential roles in retinal morphology, synaptic development, and physiology. Since TPBG has never been thoroughly examined in RBCs, we sought to characterize its expression and distribution in both the adult and developing mouse retina, and in wildtype and TRPM1 knockout retina.

2. Methods

Antibody characterization

Rabbit anti-5T4 (anti-TPBG-CT) (1:500 [immunofluorescence], 1:5000 [immunoblot]; Abcam; Cambridge, UK; Cat# ab129058; RRID: AB_11144484) is a monoclonal antibody targeting a 15-amino acid synthetic peptide immunogen from amino acids 385–420 of human TPBG, which correspond to amino acids 391–426 of mouse TPBG with 100% sequence identity (BLAST; NCBI; Bethesda, MD). TPBG immunoreactivity was verified by the manufacturer via immunoblot of rat brain, HeLa cell, and HT-1376 cell lysates, and immunoprecipitation from MCF-7 cell lysates and detected broad bands of glycosylated proteins at 70–80 kDa (manufacturer information).

Rabbit anti-5T4 (anti-TPBG-NT) (1:1000; Thermo Fisher Scientific; Waltham, MA, USA; Cat# MA5-32120; RRID: AB_2801549) is a monoclonal antibody raised against amino acids 80–240 of human TPBG, which correspond to amino acids 80–246 of mouse TPBG with 78% sequence identity (BLAST; NCBI; Bethesda, MD). The manufacturer detected a band of glycosylated TPBG at 70–80 kDa via immunoblot of MCF-7 lysate.

Sheep anti-5T4 (anti-TPBG-NT-pAb) (1:500; R&D Systems; Minneapolis, MN, USA; Cat# AF5049; RRID: AB_2272148) is a polyclonal antibody raised against amino acids 30 to 361 of mouse TPBG. The manufacturer used flow cytometry and immunocytochemistry to detect TPBG in the membranes of retinoic acid-treated D3 mouse cell lines (manufacturer information). We confirmed specificity of all three antibodies by immunoprecipitation

followed by immunoblotting from wild type mouse retinal lysate and TPBG-transfected HEK293 cells, with all antibodies detecting a broad band around 72 kDa.

Mouse anti-PKCα (1:5000; Sigma-Aldrich; St. Louis, MO, USA; Cat# P5704; RRID: AB_477375) is a monoclonal antibody that recognizes an epitope between amino acids 296–317 on the hinge region of mouse PKCα. The manufacturer detected bands at 80 kDa in immunblots of lysates from SH-SY5Y, SK-N-SH, COS7, and PC12 cell lines (manufacturer information), and we have verified this antibody by immunoblots of retinal lysates from wild type and PKCα knockout mice.

Mouse anti-CACNA1S (1:4000; Abcam; Cat# ab2862; RRID: AB_2069567) is a monoclonal antibody raised against full-length native rabbit CACNA1S subunit purified from the rabbit muscle T-tubule dihydropyridine receptor.

Mouse anti-CtBP2 (1:4000; BD Biosciences; San Jose, CA, USA; Cat# 612044; RRID: AB_399431) is a monoclonal antibody that binds an epitope within amino acids 361–445 the transcription factor CtBP2. The manufacturer used western blot analysis on BC3H1 cell lysates and detected a band at 48 kDa (manufacturer information). This antibody also reacts with ribeye, a component of synaptic ribbons (Schmitz, Königstorfer, & Südhof, 2000), and produces strong immunoreactivity in both nuclei and synaptic ribbons in wild type mouse retina sections.

Mouse anti-calretinin (1:25; Santa Cruz Biotechnology; Dallas, TX, USA; Cat# sc-365956; RRID: AB_10846469) is a monoclonal antibody that recognizes an epitope between amino acids 2–27 at the N-terminus of human calretinin. The manufacturer used western blot analysis to detect bands between 23 and 34 kDa from human cerebellum, human brain, human adrenal gland, and rat cerebellum lysates (manufacturer information). We confirmed specificity by labeling wild type mouse retina sections and detected the characteristic three-band pattern of calretinin in the IPL.

Sheep anti-TRPM1 (1:2000) is a polyclonal antibody raised against a fragment of recombinant polypeptide corresponding to amino acids 1423–1622 of mouse TRPM1 (Y Cao, Posokhova, & Martemyanov, 2011). We received this antibody from Kirill Martemyanov.

Mouse anti-β-actin (1:2500; Cell Signaling Technology; Danvers, MA, USA; Cat# 8H10D10; RRID: AB_2242334) is a monoclonal antibody that was verified in this study by immunoblot of wild type whole retinal lysates from mice at different developmental stages and shown to produce bands at ~42 kDa. The manufacturer used western blot analysis of extracts from COS, HeLa, C2C12, C6, and CHO cells to confirm immunoreactivity for β-actin.

The secondary antibodies used were AF488 anti-rabbit (1:1000; Jackson ImmunoResearch Labs; West Grove, PA, USA; Cat# 111-545-144; RRID: AB_2338052), AF488 anti-sheep (1:1000; Jackson ImmunoResearch Labs; Cat# 713-545-147; RRID: AB_2340745), Cy3 anti-mouse (1:1000; Jackson ImmunoResearch Labs; Cat# 115-165-003; RRID: AB_2338680), 680RD anti-rabbit (1:15000; LI-COR Biosciences; Lincoln, NE, USA; Cat#

925-68071; RRID: AB_2721181), 680RD anti-goat (sheep) (1:15000; LI-COR Biosciences; Cat# 925-68074; RRID: AB_2650427), and 800CW anti-mouse (1:15000; LI-COR Biosciences; Cat# 925-32212; RRID: AB_2716622).

Expression vector

The TPBG expression vector contains full-length mouse TPBG cDNA (NM_011627.4) inserted into the pCMV-sport6 plasmid (Thermo Fisher Scientific; Cat# 12209) provided by the PlasmID Repository (Clone ID: MmCD00318800; Species ID: 21983; Harvard Medical School; Boston, MA, USA).

Mice

Wild type mice used were C57BL/6J (Jackson Laboratory; Bar Harbor, ME, USA; Cat#000664, RRID: IMSR_JAX:000664). The TRPM1 knockout mice were $TRPM1^{tm1Lex}$ (Texas A&M Institute of Genomic Medicine; College Station, TX, USA; Morgans et al., 2009). Mice of both sexes were used, and all mice were maintained on a 12-hour light/dark cycle and provided food and water ad libitum. Adult mice were 3–6 months old and postnatal mice were 0 to 13 days old. All animal procedures were in accordance with the National Institutes of Health guidelines and approved by the Oregon Health and Science University Institutional Animal Care and Use Committee.

HEK293 cell transfection

HEK293 cells (ATCC Cat# CRL-1573) were maintained at 37 C and 5% CO_2 in 1X DMEM medium (Thermo Fisher Scientific; Waltham, MA, USA; Cat# 11995-065, RRID: CVCL_0045) supplemented with 10% fetal bovine serum (Gemini Bio-Products Cat# 900-108) and 1% Pen/Strep (Thermo Fisher Scientific; Cat# 15140-122). For protein expression, approximately 10^5 cells were plated on coverslips (Thermo Fisher Scientific; Cat# 12-540-80) coated with poly-l-lysine (Sigma-Aldrich; Cat# P4704) in a 24-well dish. The next day, 0.2 ng of the pCMV-TPBG-sport6 vector was transfected using the Effectene transfection reagent kit (Qiagen; Venlo, Netherlands; Cat# 301525), and expression was assessed by immunostaining approximately 24 hours after transfection.

Immunostaining transfected HEK293 cells

Fixed and permeabilized cells: Cells grown on glass cloverslips were washed with 0.1 M $+Mg^{2+}/+Ca^{2+}$ phosphate buffered saline, pH 7.4 (PBS), fixed for 10 min in 4% paraformaldehyde (PFA), and then washed again with PBS. The cells were permeabilized and blocked by incubation with antibody incubation solution (AIS: 3% normal horse serum, 0.5% Triton X-100, 0.025% NaN_3 in PBS) for 30–60 min. Primary antibody diluted in AIS was added to the cells and incubated at room temperature for 1 hr, before being removed and the cells washed with PBS. Secondary antibody, also diluted in AIS, was added at room temperature for 1 hr, then removed. 1X DAPI was added to the coverslips for 1 min, before being washed off with PBS. The coverslips were then mounted on Super-Frost glass slides in Lerner Aqua-Mount (Thermo Fisher Scientific; Cat# 13800) and sealed.

Live cells: Cells grown on coverslips were washed with PBS and given fresh DMEM medium. Primary antibody was added directly to the medium, and the cells were placed on ice for 1 hr, after which they were washed with PBS, fixed with 4% PFA, and permeabilized with AIS. The remaining steps were identical to the previous section.

Tissue preparation for immunofluorescence

Mouse eyecups were prepared from freshly dissected eyes by cutting behind the ora serrata and removing the cornea and lens. Eyecups were fixed for 30 min by immersion in 4% PFA in PBS. The fixed eyecups were washed in PBS and then cryoprotected via sequential immersion in 10, 20, and 30% sucrose in PBS. The tissue was embedded in Tissue-Tek O.C.T. Compound (Sakura Finetek; Tokyo, Japan; Cat# 4583) and stored frozen at −80 C until sectioning. Sections were cut at 20 μm thickness on a cryostat and then mounted onto Super-Frost glass slides. The slides were air dried and stored at −20 C.

Immunostaining retina sections

Retina sections were thawed and then blocked and permeabilized by incubation at room temperature for 60 min in AIS, and then were incubated in primary antibodies for 1 hr at room temperature. After washing with PBS, the sections were incubated in secondary antibodies diluted in AIS for 1 hr at room temperature. Finally, the sections were incubated for 1 min with 1X DAPI. The slides were washed again in PBS and then mounted with Lerner Aqua-Mount. For the anti-TPBG-CT and anti-TPBG-NT antibodies, retina sections were post-fixed for 10 min in 4% PFA before the blocking and permeabilization step as this was found to improve the immunofluorescence with these antibodies.

Confocal imaging

Immunofluorescence images were taken with a Leica TCS SP8 X white light laser confocal microscope (Leica; Wetzlar, Germany) using a Leica HC PL APO CS2 63x/1.40 oil immersion objective (Leica; Cat# 15506350) and Leica HyD hybrid detectors. Laser lines used were DAPI (405 nm), AF488 (499 nm), Cy3 (554 nm), and AF594 (598 nm). Detection windows used were DAPI (415–489 nm), AF488 (509–544 nm), Cy3 (564–758 nm), and AF594 (608–766 nm). Z-projections intended for comparison were processed in LAS X using identical tissue thickness. See Figure Legends for image stack number and Z-step thickness for each image. Brightness and contrast were adjusted equally across comparison groups using Leica LAS X or ImageJ (Rueden et al., 2017). The ImageJ “Smooth” tool was used to remove graininess from images.

Quantification of immunofluorescence was achieved by preparing slides with four wild type and four TRPM1 knockout sections and staining them simultaneously. Images were taken of each section with identical laser and detector settings. Brightness and contrast were corrected equally across images using ImageJ. For each section, DAPI and PKCα counterstaining was used to create 20 μm × 20 μm regions in the OPL, the middle of the IPL, and sublamina 5 of the IPL. Two such regions were averaged per layer for each image. Fluorescence intensity was quantified by normalizing the mean intensity of each region to that of a 20 μm × 20 μm region of background fluorescence in the ONL.

Immunoblotting

Retinas were extracted from freshly dissected eyes, suspended in chilled lysis buffer (50 mM Tris pH 7.4, 150 mM NaCl, 1 mM EDTA, 1% Triton X-100, 1% deoxycholate, 0.1% SDS) with 1X protease/phosphatase inhibitor cocktail (Cell Signaling Technology; Danvers, MA, USA; Cat# 5872) and homogenized with a Teflon-glass homogenizer. The lysate was centrifuged for 15 min at 16,400 rpm and 4 C, and the pellet was discarded. Lysates were stored at −20°C. Retinal lysates were diluted to 1μg/μl in lysis buffer and brought to 1X NuPAGE LDS Sample Buffer (Thermo Fisher Scientific; Cat# NP0007) and 1X NuPAGE Sample Reducing Agent (Thermo Fisher Scientific; Cat# NP0009). Pre-cast NuPAGE 1mm 4–12% Bis-Tris gels (Thermo Fisher Scientific; Cat# NP0322BOX) were loaded and run at 200 V and 140 mA for 55 min in 1X NuPAGE BOLT SDS Running Buffer (Thermo Fisher Scientific; Cat# B0001). Proteins were transferred onto PVDF membranes using a semi-dry transfer system and 2X NuPAGE Transfer Buffer (Thermo Fisher Scientific; Cat# NP00061) with 10% MeOH at 45 mA for 2 hrs, or a wet transfer system and 1X NuPAGE Transfer Buffer with 5% MeOH at 300mA for 2 hrs. The membranes were then rinsed with methanol and blocked for 1 hr in Odyssey Blocking Buffer TBS (LI-COR Biosciences; Cat# 927–50003) on a shaker at room temperature, before being incubated in primary antibody diluted in Odyssey buffer at 4°C overnight. The membranes were washed 3×5 min in TBST (Tris-buffered saline with 0.1% Tween-20), then incubated in secondary antibody diluted in Odyssey buffer for 1 hr at room temperature before being washed 3×5 min in TBST and left to dry. The dry blots were imaged using a LI-COR Odyssey CLx Imaging System at 700 and 800 nm.

3. Results

TPBG is expressed in the dendrites and axon terminals of rod bipolar cells.

Two rabbit monoclonal antibodies against different epitopes of human TPBG were used to localize TPBG in mouse retina. The first, anti-TPBG-CT, reacts with an epitope near the PDZ-interacting motif of TPBG's intracellular C-terminal tail, while the second, anti-TPBG-NT, binds within the extracellular N-terminal leucine-rich repeat (LRR) domain of TPBG. On immunoblots of retinal lysates, both antibodies label a single, broad band centered around 70 kDa, consistent with the size of glycosylated TPBG. Wild type mouse retina sections were labeled with either anti-TPBG-CT or anti-TPBG-NT, and the nuclear stain DAPI was used to identify the different retinal layers. The two antibodies gave indistinguishable results, further supporting the specificity of each antibody for TPBG. Immunofluorescent labeling with either anti-TPBG-CT (Figure 1a–c) or anti-TPBG-NT (Figure 1d–f) revealed strong immunoreactivity in the OPL and in two bands in the IPL, one in the middle of the IPL (arrows) and the other at the innermost IPL. In the inner nuclear layer (INL), both TPBG antibodies label putative RBC cell bodies near the OPL as well as sparse cell bodies near the IPL (asterisks). Immunofluorescent double-labeling of TPBG and PKCα confirmed localization of TPBG to RBCs in retina sections (Figure 1b, c, e, and f). TPBG immunofluorescence can be seen throughout the dendritic branches of RBCs in the OPL, as well as weaker labeling of their cell bodies in the outer INL (Figures 1b and e), and their axon terminals in the IPL (Figure 1c and f). In the OPL, anti-PKCα labels RBC cell bodies and dendrites, with the densest labeling occurring in the proximal dendrites close to

the cell bodies. TPBG antibodies labeled the distal RBC dendrites more intensely than anti-PKCα. In the IPL, nearly complete co-localization of TPBG and PKCα in sublamina 5 confirms localization of TPBG to RBC axon terminals. Finally, a sparse group of cells was also strongly reactive with anti-TPBG antibodies (Figure 1 a, c, d, and f), with cell bodies (asterisks) localized to the inner INL and projections to a dense, narrow layer in the center of the IPL (arrows).

In a dissociated retina preparation, anti-TPBG-CT (Figure 2a) and anti-TPBG-NT (Figure 2b) labeled PKCα-positive RBCs and, very rarely, a presumed amacrine cell (not shown). TPBG labeling of dissociated RBCs is more widespread throughout the cell compared to labeling of RBCs in retinal sections. This is likely due to disruption of protein synthesis and distribution of immunoreactivity caused by the dissociation procedure.

To examine the dendritic distribution of TPBG in the mouse OPL, we compared TPBG-CT immunofluorescence with that of GPR179 and CtBP2 (Figure 3). GPR179 is localized exclusively to the dendritic tips of ON-bipolar cells where it is responsible for anchoring the RGS7-Gβ5 complex to the postsynaptic membrane (Orhan et al., 2013; Orlandi, Cao, & Martemyanov, 2013; Tayou et al., 2016) in proximity to mGluR6 (Morgans et al., 2007; Ray et al., 2014). To label GPR179, we used a monoclonal antibody to CACNA1S ($Ca_V1.1$) that has been shown to strongly cross-react with retinal GPR179 in the tips of ON-bipolar cell dendrites (Hasan, Ray, & Gregg, 2016). TPBG-labeled puncta do not overlap the putative GPR179 puncta at the very tips of the RBC dendrites, but do closely associate with them (Figure 3a). In the OPL, antibodies against CtBP2 label ribeye, a protein component of horseshoe-shaped synaptic ribbons in both cone and rod synaptic terminals (Schmitz et al., 2000). TPBG immunofluorescent puncta lie within the concavity of a subset of horseshoe-shaped ribbons (Figure 3b, asterisks), indicating localization to RBC invaginating dendrites. Taken together, the double-labeling with these synaptic markers is consistent with the presence of TPBG in distal RBC dendrites, but TPBG could not be clearly detected in the dendritic tips using immunofluorescence.

TPBG is localized to the plasma membrane in live transfected HEK293 cells.

Based on its structure and similarities with other LRR proteins, TPBG is expected to be oriented in the plasma membrane with its N-terminal LRRs facing the extracellular space and its C-terminus in the cytoplasm. Since immunofluorescence in retina sections could not clearly reveal the distribution of TPBG in RBCs, and because of disruption of surface proteins in dissociated preparations, we aimed to better visualize the distribution and membrane orientation of TPBG using HEK293 cells. HEK293 cells were transfected with full-length mouse TPBG and both fixed and live cells were labeled with a sheep polyclonal antibody against the N-terminal extracellular domain (anti-TPBG-NT pAb) (Figure 4). In fixed and permeabilized cells, the antibody labeled plasma membrane and cytoplasmic structures (Figure 4a). In live cells, the antibody only has access to the extracellular surface; thus, the labeling of live cells (Figure 4b) confirms the predicted orientation of TPBG with the N-terminal, LRR domain facing the extracellular space.

TPBG is present in sublamina 2/3 of the IPL.

The IPL is divided into two layers corresponding to inputs from ON and OFF bipolar cells, and can be further subdivided into five sublamina (2 OFF sublamina and 3 ON sublamina) based on labeling with immunofluorescence markers. One such IPL marker, calretinin, labels three distinct synaptic layers in the IPL corresponding to the sublamina 1/2, 2/3, and 3/4 boundaries (Haverkamp & Wässle, 2000). Antibodies against TPBG labeled a dense synaptic layer in the middle of the IPL (Figure 5; arrows), overlapping with calretinin at the boundary between sublamina 2 and 3 between the ON and OFF regions of the IPL.

TPBG immunofluorescence is reduced in TRPM1 knockout retinas.

Knockout of TRPM1 abolishes the RBC light response and significantly reduces PKCα-dependent phosphorylation in the retina (Wakeham et al., 2019). TPBG shows PKCα-dependent phosphorylation, so to examine whether the loss of TRPM1 alters TPBG localization or expression, we compared wild type and TRPM1 knockout retinas by immunofluorescent labeling and immunoblotting retinal lysates with anti-TPBG-CT. To quantify TPBG expression in retina sections retinal layers were identified using DAPI and PKCα counterstaining and fluorescence intensity from different retinal layers was normalized to the nonspecific background fluorescence in the outer nuclear layer. In TRPM1 knockout retina, TPBG immunoreactivity in RBCs was significantly reduced compared to wild type, but the labeling in processes in sublamina 2/3 of the IPL were unaffected (Figure 6a and b). For the immunoblot analysis, bands at around 70 kDa corresponding to TPBG were normalized to β-actin bands within each sample to control for changes in total protein between samples, and the knockout was normalized to the wild type. Surprisingly, there was no change in total TPBG levels as assessed via immunoblot analysis (Figure 6c and d).

TPBG expression in the retina increases the day before eye opening.

To analyze the time-course of TPBG expression in the developing mouse retina, retinal lysates were extracted at different postnatal (P) days and probed via immunoblot with antibodies to TRPM1 and anti-TPBG-CT (Figure 7a) or anti-TPBG-NT (not shown; identical pattern). Both TPBG antibodies detected a significant increase in retinal TPBG expression the day before eye opening, which occurred between P12 and P13 in all three litters used, and is concomitant with an increase in the expression of TRPM1. Quantification of TPBG band intensities normalized to β-actin and to P0 (Figure 7b) showed that TPBG expression remains stable until P11, then increases approximately 10-fold by P12 and remains elevated. Quantification of TRPM1 band intensities (Figure 7c) revealed a similar pattern. The increase in TPBG expression around eye opening was also apparent in sections made from postnatal mouse retinas labeled with the anti-TPBG antibodies (only anti-TPBG-CT shown). TPBG immunofluorescence was undetectable in the P0 retina (not shown). In the P6 retina, the TPBG-positive cell bodies in the inner INL and labeling in sublamina 2/3 of the IPL are just visible (Figure 7d; arrows). By P11, TPBG can be faintly seen in RBC dendrites in the OPL (Figure 7e; arrowheads), but is still mostly absent from RBC axon terminals in sublamina 5 of the IPL. At P12 (Figure 7f), TPBG immunofluorescence in the OPL has dramatically increased, as has RBC axon terminal labeling in the IPL. By P13

(Figure 7g), after eye opening, RBC dendrites in the OPL are clearly visible when labeled for TPBG.

4. Discussion

In this study, we have described the localization and expression patterns of TPBG in the mouse retina using two antibodies against intracellular and extracellular epitopes of TPBG. We found TPBG immunofluorescence primarily in the dendrites and axon terminals of RBCs, in cell bodies adjacent to the INL, and in processes that stratify in the middle of the IPL (Figures 1 and 2). In the OPL, TPBG labeling was closely associated with the RBC dendrites but was not clearly and consistently detected in the dendritic tips (Figure 3), localizing near, but not overlapping markers of RBC dendritic tips and rod synaptic ribbons. In HEK293 cells, transfected TPBG was primarily localized to the cell membrane with the N-terminal domain facing the extracellular space (Figure 4). In sublamina 5 of the IPL, antibodies against TPBG label RBC axon terminals, overlapping strongly with PKCα.

TPBG structure and function.

The N-terminal extracellular region of TPBG contains a heavily glycosylated (Shaw et al., 2002) LRR domain – a common site of protein-protein interactions (Zhao et al., 2014) Several similarly structured transmembrane proteins have recently been identified as vital for the development of the rod-RBC synapse or for localization of RBC synaptic transduction components. ELFN1, a synaptic adhesion LRR protein expressed in rod photoreceptors, forms trans-synaptic complexes with mGluR6 in RBC dendrites, and is required for the development of a functional synapse (Yan Cao et al., 2015; Dunn, Patil, Cao, Orlandi, & Martemyanov, 2018). Two other synaptic LRR proteins, LRIT3 and nyctalopin, are required for the localization of TRPM1 to the tips of ON bipolar cell dendrites (Y Cao et al., 2011; Neuillé et al., 2017, 2015; Pearring et al., 2011). Our immunofluorescence data shows that TPBG is localized to RBC dendrites and in the RBC axon terminals. Structural similarities between TPBG and other LRR proteins suggest a possible role in the development or maintenance of RBC synapses.

The C-terminal intracellular region of TPBG is capped with a class 1 PDZ-interacting motif containing two serines (S422 and S424) that we have shown to be targets of PKCα-dependent phosphorylation (Wakeham et al., 2019). Phosphorylation of PDZ-interacting motifs has been shown to regulate binding to PDZ domains. For example, the C-terminal PDZ-interacting motifs of NMDA receptor subunits NR2A and NR2B end with the amino acids SDV, and phosphorylation of the serine blocks binding of the receptor to the PDZ domain of PSD95 (Chung, Huang, Lau, & Huganir, 2004). The PDZ-interacting motif of TPBG also ends with the amino acids SDV, but it is not known what PDZ domain proteins may interact with C-terminal TPBG in the retina. In other tissues, TPBG has been demonstrated by yeast two-hybrid screening to bind to the PDZ domain of GIPC1, a scaffolding protein that regulates cell surface expression of GPCRs (Awan et al., 2002) and that is expressed in RBCs (Shekhar et al., 2016). Through interactions with scaffolding proteins like GIPC1, TPBG could regulate signal transduction by interacting with RGS

proteins (De Vries, Lou, Zhao, Zheng, & Farquhar, 1998), and alter receptor targeting (Hu et al., 2003) or degradation (Wieman et al., 2009).

TRPM1-dependent distribution of TPBG in RBCs.

TRPM1 is the mGluR6-coupled nonspecific cation channel responsible for the depolarizing light response in RBCs (Koike et al., 2010; Morgans et al., 2009; Shen et al., 2009), and knockout of TRPM1 abolishes the RBC light response. We have previously shown that loss of TRPM1 in the mouse retina significantly reduces PKCα phosphorylation in the OPL (Wakeham et al., 2019), which may affect the expression or distribution of PKCα-dependent phosphoproteins such as TPBG. Immunofluorescent labeling of TPBG in RBCs by both antibodies was markedly affected by the loss of TRPM1, with reduced immunofluorescence in TRPM1 knockout retina compared to wild type (Figure 6). In contrast, TPBG expression in sublamina 2/3 of the IPL was unaffected, and the total amount of TPBG detected by immunoblot was unchanged. Together, our immunofluorescence and immunoblot results suggest that, when TPBG immunofluorescence in RBCs is reduced in the TRPM1 knockout, either TPBG is more diffusely distributed throughout the cells or antibody binding is occluded, potentially by light-dependent or phosphorylation-dependent protein interactions.

TPBG expression in the developing retina.

During retinal development, TPBG expression is undetectable by immunofluorescence at birth. The presence of TPBG in the putative amacrine cells is visible by P6, and in RBCs by P11. RBC expression increases dramatically between P11 and P12, just prior to eye opening (Figure 7). This pattern of increased expression approaching eye opening matches that of TRPM1, and is coincident with the gene expression patterns of many other proteins associated with the final stages of development of RBC signal transduction machinery and establishment of the rod to RBC synapse (Blackshaw et al., 2004; Dorrell, Aguilar, Weber, & Friedlander, 2004; Mu et al., 2001; Zhang, Kolodkin, Wong, & James, 2017). In embryonic development, TPBG alters Wnt and cytokine signaling to modulate cytoskeletal rearrangement and cell morphology (Kagermeier-Schenk et al., 2011; McGinn et al., 2012; Southgate et al., 2010). In the developing mouse retina, Wnt signaling between rods and RBCs is required for functional synaptic targeting and OPL lamination, and knockout of Wnt5 resulted in rod/RBC mistargeting and the formation of ectopic OPL (Sarin et al., 2018). Similarly, Ccl5-mediated chemokine signaling was found to be required for RBC axon terminal targeting to AII amacrine cell dendrites in the IPL (Duncan et al., 2018), suggesting that both Wnt- and chemokine-dependent mechanisms are active during RBC dendritic and axonal development. No relationship between TPBG and Wnt or chemokine signaling in the retina have yet been shown. However, as TPBG expression in RBCs increases concurrently with the activation of developmental processes dependent on these signaling pathways, and TPBG regulates both Wnt and chemokine signaling in other tissues, TPBG might be modulating similar signaling pathways in the retina.

TPBG-positive amacrine cells and IPL lamination.

We found that both antibodies against TPBG label an uncharacterized group of cell bodies in the INL and a dense synaptic layer between the ON and OFF sublamina in the IPL (Figure 5). A TPBG-positive amacrine cell with cell bodies near the IPL and dense processes

stratifying in the middle of the IPL was first identified in a study focusing on TPBG in mouse olfactory bulb granule cells (Imamura et al., 2006), and a TPBG-positive amacrine cell type was identified by single-cell transcriptome analysis of retina (Macosko et al., 2015). TPBG-promoter-driven expression of GFP labels a morphologically similar type of amacrine cell (Gensat Retina Project; www.gensat.org/retina.jsp). Based on similarities in cell body distribution and IPL lamination, we hypothesize that the TPBG-positive cell bodies and 2/3 sublamina labeling both come from the Type 47 (ac53–59) amacrine cell identified via connectomic reconstruction of the IPL, which was shown to receive inputs from cone bipolar cell 5D (XBC) and project outputs to two distinct populations of ganglion cells between the ON and OFF sublamina (Helmstaedter et al., 2013). The sparse distribution and dense lamination, combined with the connectome data from Helmstaedter et al., indicates that this TPBG-positive amacrine cell may have a medium-to-wide dendritic field and be coupled to both the ON and OFF pathways. While this evidence suggests that immunofluorescence from cell bodies in the INL and in the middle of the IPL come from the same uncharacterized amacrine cells, we cannot rule out potential contributions from other amacrine cell or ganglion cell synapses.

Summary

This study found that TPBG is localized to the dendrites and axon terminals of RBCs and the cell bodies and dendritic projections of an uncharacterized group of potential amacrine cells in mouse retina. TPBG immunofluorescence, but not total protein, was strongly reduced in the absence of TRPM1, possibly due to changes in protein distribution or protein interactions between knockout and wild type retina. TPBG is expressed in the developing and adult retina, suggesting a potential role both in the development and maintenance of RBC cellular physiology before and after eye opening. Based on TPBG's role in embryonic development, cancer pathogenesis, and the development and morphology of olfactory bulb interneurons, and its structural similarities to other synaptic LRR proteins, it is reasonable to predict that TPBG may be involved in the development and maintenance of RBC synaptic morphology and function.

Acknowledgments:

The authors would like to thank Tammie L Haley for providing retina sections for immunofluorescent labeling. This work was supported by National Institutes of Health grants R01EY022369 and 5P30EY010572.

Abbreviations:

CtBP2	C-terminal binding protein 2
GCL	ganglion cell layer
GPR179	G protein-coupled receptor 179
INL	inner nuclear layer
IPL	inner plexiform layer
LRR	leucine-rich repeat

OPL	outer plexiform layer
PKCα	protein kinase C-alpha
RBC	rod bipolar cell
TPBG	trophoblast glycoprotein
TRPM1	transient receptor potential cation channel subfamily M member 1

References

Abd-El-Barr MM, Pennesi ME, Saszik SM, Barrow AJ, Lem J, Bramblett DE, … Wu SM (2009). Genetic Dissection of Rod and Cone Pathways in the Dark-Adapted Mouse Retina. Journal of Neurophysiology, 102(3), 1945–1955. 10.1152/jn.00142.2009 [PubMed: 19587322]

Awan A, Lucic MR, Shaw DM, Sheppard F, Westwater C, Lyons SA, & Stern PL (2002). 5T4 Interacts with TIP-2/GIPC, a PDZ Protein, with Implications for Metastasis. Biochemical and Biophysical Research Communications, 290(3), 1030–1036. 10.1006/bbrc.2001.6288 [PubMed: 11798178]

Barrow KM, Ward CM, Rutter J, Ali S, & Stern PL (2005). Embryonic expression of murine 5T4 oncofoetal antigen is associated with morphogenetic events at implantation and in developing epithelia. Developmental Dynamics : An Official Publication of the American Association of Anatomists, 233(4), 1535–1545. 10.1002/dvdy.20482 [PubMed: 15977177]

Berntson A, Smith RG, & Taylor WR (2004). Transmission of single photon signals through a binary synapse in the mammalian retina. Visual Neuroscience, 21(5), 693–702. 10.1017/S0952523804215048 [PubMed: 15683557]

Blackshaw S, Harpavat S, Trimarchi J, Cai L, Huang H, Kuo WP, … Cepko CL (2004). Genomic analysis of mouse retinal development. PLoS Biology, 2(9), E247. 10.1371/journal.pbio.0020247

Cao Y, Posokhova E, & Martemyanov KA (2011). TRPM1 Forms Complexes with Nyctalopin In Vivo and Accumulates in Postsynaptic Compartment of ON-Bipolar Neurons in mGluR6-Dependent Manner. Journal of Neuroscience, 31(32), 11521–11526. 10.1523/JNEUROSCI.1682-11.2011 [PubMed: 21832182]

Cao Yan, Sarria I, Fehlhaber KE, Kamasawa N, Orlandi C, James KN, … Martemyanov KA (2015). Mechanism for Selective Synaptic Wiring of Rod Photoreceptors into the Retinal Circuitry and Its Role in Vision. Neuron, 87(6), 1248–1260. 10.1016/j.neuron.2015.09.002 [PubMed: 26402607]

Chung HJ, Huang YH, Lau L-F, & Huganir RL (2004). Regulation of the NMDA Receptor Complex and Trafficking by Activity-Dependent Phosphorylation of the NR2B Subunit PDZ Ligand. Journal of Neuroscience, 24(45), 10248–10259. 10.1523/JNEUROSCI.0546-04.2004 [PubMed: 15537897]

De Vries L, Lou X, Zhao G, Zheng B, & Farquhar MG (1998). GIPC, a PDZ domain containing protein, interacts specifically with the C terminus of RGS-GAIP. Proceedings of the National Academy of Sciences of the United States of America, 95(21), 12340–12345. 10.1073/pnas.95.21.12340 [PubMed: 9770488]

Dorrell MI, Aguilar E, Weber C, & Friedlander M. (2004). Global gene expression analysis of the developing postnatal mouse retina. Investigative Ophthalmology and Visual Science, 45(3), 1009–1019. 10.1167/iovs.03-0806 [PubMed: 14985324]

Duncan DS, Weiner RL, Weitlauf C, Risner ML, Roux AL, Sanford ER, … Sappington RM (2018). CCL5 mediates proper wiring of feedforward and lateral inhibition pathways in the inner retina. Frontiers in Neuroscience, 12, 702 10.3389/fnins.2018.00702 [PubMed: 30369865]

Dunn HA, Patil DN, Cao Y, Orlandi C, & Martemyanov KA (2018). Synaptic adhesion protein ELFN1 is a selective allosteric modulator of group III metabotropic glutamate receptors in trans. Proceedings of the National Academy of Sciences, 115(19), 5022–5027. 10.1073/pnas.1722498115

Euler T, Haverkamp S, Schubert T, & Baden T. (2014). Retinal bipolar cells: elementary building blocks of vision. Nature Publishing Group, 15(8), 507–519. 10.1038/nrn3783

Hasan N, Ray TA, & Gregg RG (2016). CACNA1S expression in mouse retina: Novel isoforms and antibody cross-reactivity with GPR179. Visual Neuroscience, 33, E009. 10.1017/S0952523816000055

Haverkamp S, & Wässle H. (2000). Immunocytochemical analysis of the mouse retina. Journal of Comparative Neurology, 424(1), 1–23. 10.1002/1096-9861(20000814)424:1<1::AID-CNE1>3.0.CO;2-V [PubMed: 10888735]

Helmstaedter M, Briggman KL, Turaga SC, Jain V, Seung HS, & Denk W. (2013). Connectomic reconstruction of the inner plexiform layer in the mouse retina. Nature, 500(7461), 168–174. 10.1038/nature12346 [PubMed: 23925239]

Hole N, & Stern PL (1988). A 72 kD trophoblast glycoprotein defined by a monoclonal antibody. British Journal of Cancer, 57(3), 239–246. 10.1038/bjc.1988.53 [PubMed: 3355761]

Hu LA, Chen W, Martin NP, Whalen EJ, Premont RT, & Lefkowitz RJ (2003). GIPC interacts with the β1-adrenergic receptor and regulates β1-adrenergic receptor-mediated ERK activation. Journal of Biological Chemistry, 278(28), 26295–26301. 10.1074/jbc.M212352200 [PubMed: 12724327]

Imamura F, Nagao H, Naritsuka H, Murata Y, Taniguchi H, & Mori K. (2006). A leucine-rich repeat membrane protein, 5T4, is expressed by a subtype of granule cells with dendritic arbors in specific strata of the mouse olfactory bulb. The Journal of Comparative Neurology, 495(6), 754–768. 10.1002/cne.20896 [PubMed: 16506198]

Kagermeier-Schenk B, Wehner D, Özhan-Kizil G, Yamamoto H, Li J, Kirchner K, … Weidinger G. (2011). Waif1/5T4 Inhibits Wnt/β-Catenin Signaling and Activates Noncanonical Wnt Pathways by Modifying LRP6 Subcellular Localization. Developmental Cell, 21(6), 1129–1143. 10.1016/j.devcel.2011.10.015 [PubMed: 22100263]

Ke J-B, Wang YV, Borghuis BG, Cembrowski MS, Riecke H, Kath WL, … Singer JH (2014). Adaptation to Background Light Enables Contrast Coding at Rod Bipolar Cell Synapses. Neuron, 81(2), 388–401. 10.1016/j.neuron.2013.10.054 [PubMed: 24373883]

King KW, Sheppard FC, Westwater C, Stern PL, & Myers KA (1999). Organisation of the mouse and human 5T4 oncofoetal leucine-rich glycoprotein genes and expression in foetal and adult murine tissues. Biochimica et Biophysica Acta (BBA) - Gene Structure and Expression, 1445(3), 257–270. 10.1016/S0167-4781(99)00055-X [PubMed: 10366710]

Koike C, Obara T, Uriu Y, Numata T, Sanuki R, Miyata K, … Furukawa T. (2010). TRPM1 is a component of the retinal ON bipolar cell transduction channel in the mGluR6 cascade. Proceedings of the National Academy of Sciences, 107(1), 332–337. 10.1073/pnas.0912730107

Macosko EZ, Basu A, Satija R, Nemesh J, Shekhar K, Goldman M, … McCarroll SA (2015). Highly Parallel Genome-wide Expression Profiling of Individual Cells Using Nanoliter Droplets. Cell, 161(5), 1202–1214. 10.1016/j.cell.2015.05.002 [PubMed: 26000488]

McGinn OJ, Marinov G, Sawan S, & Stern PL (2012). CXCL12 receptor preference, signal transduction, biological response and the expression of 5T4 oncofoetal glycoprotein. Journal of Cell Science, 125(22), 5467–5478. 10.1242/jcs.109488 [PubMed: 22956548]

Morgans CW, Liu W, Wensel TG, Brown RL, Perez-Leon JA, Bearnot B, & Duvoisin RM (2007). Gβ5-RGS complexes co-localize with mGluR6 in retinal ON-bipolar cells. European Journal of Neuroscience, 26(10), 2899–2905. 10.1111/j.1460-9568.2007.05867.x [PubMed: 18001285]

Morgans CW, Zhang J, Jeffrey BG, Nelson SM, Burke NS, Duvoisin RM, & Brown RL (2009). TRPM1 is required for the depolarizing light response in retinal ON-bipolar cells. Proceedings of the National Academy of Sciences of the United States of America, 106(45), 19174–19178. 10.1073/pnas.0908711106 [PubMed: 19861548]

Mu X, Zhao S, Pershad R, Hsieh TF, Scarpa A, Wang SW, … Klein WH (2001). Gene expression in the developing mouse retina by EST sequencing and microarray analysis. Nucleic Acids Research, 29(24), 4983–4993. 10.1093/nar/29.24.4983 [PubMed: 11812828]

Neuillé M, Cao Y, Caplette R, Guerrero-Given D, Thomas C, Kamasawa N, … Zeitz C. (2017). LRIT3 Differentially Affects Connectivity and Synaptic Transmission of Cones to ON-and OFF-Bipolar Cells. Investigative Ophthalmology Visual Science, 58(3), 1768 10.1167/iovs.16-20745 [PubMed: 28334377]

Neuillé M, Morgans CW, Cao Y, Orhan E, Michiels C, Sahel J-A, … Zeitz C. (2015). LRIT3 is essential to localize TRPM1 to the dendritic tips of depolarizing bipolar cells and may play a role

in cone synapse formation. European Journal of Neuroscience, 42(3), 1966–1975. 10.1111/ejn.12959 [PubMed: 25997951]

Orhan E, Prézeau L, El Shamieh S, Bujakowska KM, Michiels C, Zagar Y, … Zeitz C. (2013). Further Insights Into GPR179: Expression, Localization, and Associated Pathogenic Mechanisms Leading to Complete Congenital Stationary Night Blindness. Investigative Ophthalmology & Visual Science, 54(13), 8010–8041. 10.1167/iovs.13-12610

Orlandi C, Cao Y, & Martemyanov KA (2013). Orphan receptor GPR179 forms macromolecular complexes with components of metabotropic signaling cascade in retina ON-bipolar neurons. Investigative Ophthalmology & Visual Science, 54(10), 7153–7161. 10.1167/iovs.13-12907 [PubMed: 24114537]

Pearring JN, Bojang P, Shen Y, Koike C, Furukawa T, Nawy S, & Gregg RG (2011). A Role for Nyctalopin, a Small Leucine-Rich Repeat Protein, in Localizing the TRP Melastatin 1 Channel to Retinal Depolarizing Bipolar Cell Dendrites. Journal of Neuroscience, 31(27), 10060–10066. 10.1523/JNEUROSCI.1014-11.2011 [PubMed: 21734298]

Pukrop T, & Binder C. (2008). The complex pathways of Wnt 5a in cancer progression. Journal of Molecular Medicine, 86(3), 259–266. 10.1007/s00109-007-0266-2 [PubMed: 17952396]

Rampino MAF, & Nawy SA (2011). Relief of Mg^{2+}-dependent inhibition of TRPM1 by PKCα at the rod bipolar cell synapse. Journal of Neuroscience, 31(38), 13596–13603. 10.1523/JNEUROSCI.2655-11.2011 [PubMed: 21940450]

Ray TA, Heath KM, Hasan N, Noel JM, Samuels IS, Martemyanov KA, … Gregg RG (2014). GPR179 Is Required for High Sensitivity of the mGluR6 Signaling Cascade in Depolarizing Bipolar Cells. Journal of Neuroscience, 34(18), 6334–6343. 10.1523/JNEUROSCI.4044-13.2014 [PubMed: 24790204]

Rueden CT, Schindelin J, Hiner MC, DeZonia BE, Walter AE, Arena ET, & Eliceiri KW (2017). ImageJ2: ImageJ for the next generation of scientific image data. BMC Bioinformatics, 18(529). 10.1186/s12859-017-1934-z

Ruether K, Feigenspan A, Pirngruber J, Leitges M, Baehr W, & Strauss O. (2010). PKC{alpha} is essential for the proper activation and termination of rod bipolar cell response. Investigative Ophthalmology & Visual Science, 51(11), 6051–6058. 10.1167/iovs.09-4704 [PubMed: 20554612]

Sampath AP, & Rieke F. (2004). Selective transmission of single photon responses by saturation at the rod-to-rod bipolar synapse. Neuron, 41(3), 431–443. 10.1016/s0896-6273(04)00005-4 [PubMed: 14766181]

Sarin S, Zuniga-Sanchez E, Kurmangaliyev YZ, Cousins H, Patel M, Hernandez J, … Zipursky SL (2018). Role for Wnt Signaling in Retinal Neuropil Development: Analysis via RNA-Seq and In Vivo Somatic CRISPR Mutagenesis. Neuron, 98(1), 1–27. 10.1016/j.neuron.2018.03.004 [PubMed: 29621482]

Schmitz F, Königstorfer A, & Südhof TC (2000). RIBEYE, a Component of Synaptic Ribbons. Neuron, 28(3), 857–872. 10.1016/s0896-6273(00)00159-8 [PubMed: 11163272]

Shaw DM, Woods AM, Myers KA, Westwater C, Rahi-Saund V, Davies MJ, … Stern PL (2002). Glycosylation and epitope mapping of the 5T4 glycoprotein oncofoetal antigen. Biochemical Journal, 363(Pt 1), 137–145. 10.1042/0264-6021:3630137 [PubMed: 11903056]

Shekhar K, Lapan SW, Whitney IE, Tran NM, Macosko EZ, Kowalczyk M, … Sanes JR (2016). Comprehensive Classification of Retinal Bipolar Neurons by Single-Cell Transcriptomics. Cell, 166(5), 1308–1323. 10.1016/j.cell.2016.07.054 [PubMed: 27565351]

Shen Y, Heimel JA, Kamermans M, Peachey NS, Gregg RG, & Nawy S. (2009). A Transient Receptor Potential-Like Channel Mediates Synaptic Transmission in Rod Bipolar Cells. Journal of Neuroscience, 29(19), 6088–6093. 10.1523/JNEUROSCI.0132-09.2009 [PubMed: 19439586]

Southgate TD, McGinn OJ, Castro FV, Rutkowski AJ, Al-Muftah M, Marinov G, … Stern PL (2010). CXCR4 Mediated Chemotaxis Is Regulated by 5T4 Oncofetal Glycoprotein in Mouse Embryonic Cells. PLoS ONE, 5(4), e9982–20. 10.1371/journal.pone.0009982 [PubMed: 20376365]

Szikra T, Trenholm S, Drinnenberg A, Jüttner J, Raics Z, Farrow K, … Roska B. (2014). Rods in daylight act as relay cells for cone-driven horizontal cell–mediated surround inhibition. Nature Publishing Group, 17(12), 1728–1735. 10.1038/nn.3852

Takahashi H, Ogawa Y, Yoshihara S, Asahina R, Kinoshita M, Kitano T, … Tsuboi A. (2016). A Subtype of Olfactory Bulb Interneurons Is Required for Odor Detection and Discrimination Behaviors. Journal of Neuroscience, 36(31), 8210–8227. 10.1523/JNEUROSCI.2783-15.2016 [PubMed: 27488640]

Tayou J, Wang Q, Jang G-F, Pronin AN, Orlandi C, Martemyanov KA, … Slepak VZ (2016). Regulator of G Protein Signaling 7 (RGS7) Can Exist in a Homo-oligomeric Form That Is Regulated by Gαo and R7-binding Protein. Journal of Biological Chemistry, 291(17), 9133–9147. 10.1074/jbc.M115.694075 [PubMed: 26895961]

Wakeham CM, Wilmarth PA, Cunliffe JM, Klimek JE, Ren G, David LL, & Morgans CW (2019b). Identification of PKCα-dependent phosphoproteins in mouse retina. Journal of Proteomics, 103423. 10.1016/j.jprot.2019.103423

Weeraratna AT, Jiang Y, Hostetter G, Rosenblatt K, Duray P, Bittner M, & Trent JM (2002). Wnt5a signaling directly affects cell motility and invasion of metastatic melanoma. Cancer Cell, 1(3), 279–288. 10.1016/s1535-6108(02)00045-4 [PubMed: 12086864]

Wieman HL, Horn SR, Jacobs SR, Altman BJ, Kornbluth S, & Rathmell JC (2009). An essential role for the Glut1 PDZ-binding motif in growth factor regulation of Glut1 degradation and trafficking. Biochemical Journal, 418(2), 345–367. 10.1042/BJ20081422 [PubMed: 19016655]

Woods SM, Mountjoy E, Muir D, Ross SE, & Atan D. (2018). A comparative analysis of rod bipolar cell transcriptomes identifies novel genes implicated in night vision. Scientific Reports, 8(1), 1–15. 10.1038/s41598-018-23901-6 [PubMed: 29311619]

Xiong W-H, Pang J-J, Pennesi ME, Duvoisin RM, Wu SM, & Morgans CW (2015). The Effect of PKCα on the Light Response of Rod Bipolar Cells in the Mouse Retina. Investigative Ophthalmology Visual Science, 56(8), 4961–4974. 10.1167/iovs.15-16622 [PubMed: 26230760]

Yoshihara S, Takahashi H, Nishimura N, Naritsuka H, Shirao T, Hirai H, … Tsuboi A. (2012). 5T4 glycoprotein regulates the sensory input-dependent development of a specific subtype of newborn interneurons in the mouse olfactory bulb. Journal of Neuroscience, 32(6), 2217–2226. 10.1523/JNEUROSCI.5907-11.2012 [PubMed: 22323733]

Yoshihara S, Takahashi H, & Tsuboi A. (2016). Molecular Mechanisms Regulating the Dendritic Development of Newborn Olfactory Bulb Interneurons in a Sensory Experience-Dependent Manner. Frontiers in Neuroscience, 9(55), 134–139. 10.3389/fnins.2015.00514

Zhang C, Kolodkin AL, Wong RO, & James RE (2017). Establishing Wiring Specificity in Visual System Circuits: From the Retina to the Brain. Annual Review of Neuroscience, 40(1), 395–424. 10.1146/annurev-neuro-072116-031607

Zhao Y, Malinauskas T, Harlos K, & Jones EY (2014). Structural insights into the inhibition of Wnt signaling by cancer antigen 5T4/Wnt-activated inhibitory factor 1. Structure (London, England : 1993), 22(4), 612–620. 10.1016/j.str.2014.01.009

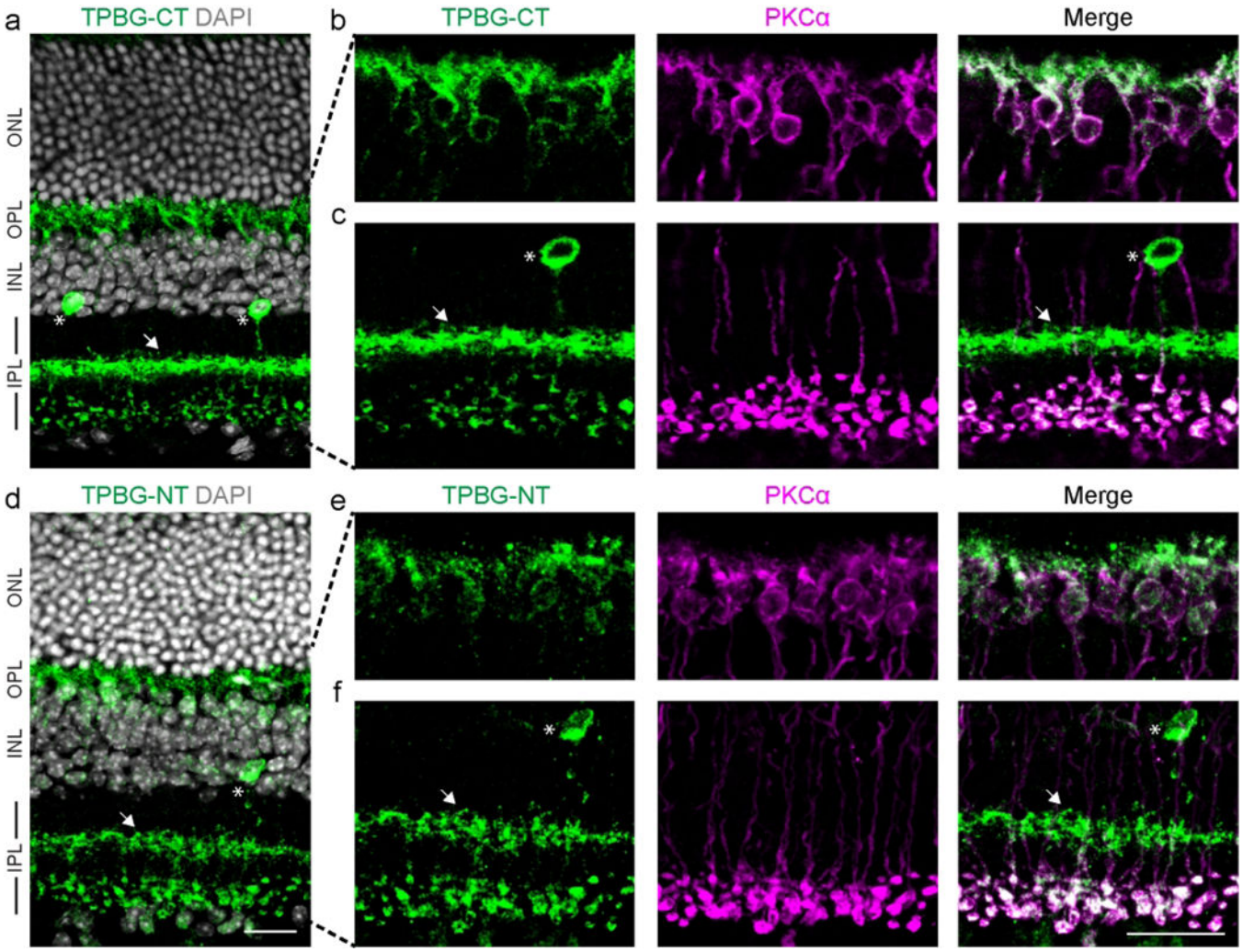

Figure 1: TPBG in the mouse retina.

Three-channel confocal microscopy of wild type retina labeled with anti-TPBG-CT (green; a-c) or anti-TPBG-NT (green, d-f). DAPI (grey; a and c) was used to highlight the layers of the neural retina and anti-PKCα (magenta; b and c [1.8X zoom of a] and e and f [1.8X zoom of d]) was used to identify RBCs. Zoomed images were cropped into OPL (top) and IPL (bottom) panels to allow for separate intensity and contrast processing. Asterisks mark TPBG-positive cell bodies in the inner INL and arrows point to processes in the middle of the IPL. Sites of co-localization appear white. For a and d, Z-projections of 9 sections were used. For b, c, e, and f, Z-projections of 4 sections were used. For all images, the Z-step distance was 0.297 μm. Scale bars: 20 μm. ONL: outer nuclear layer; OPL: outer plexiform layer; INL: inner nuclear layer; IPL: inner plexiform layer.

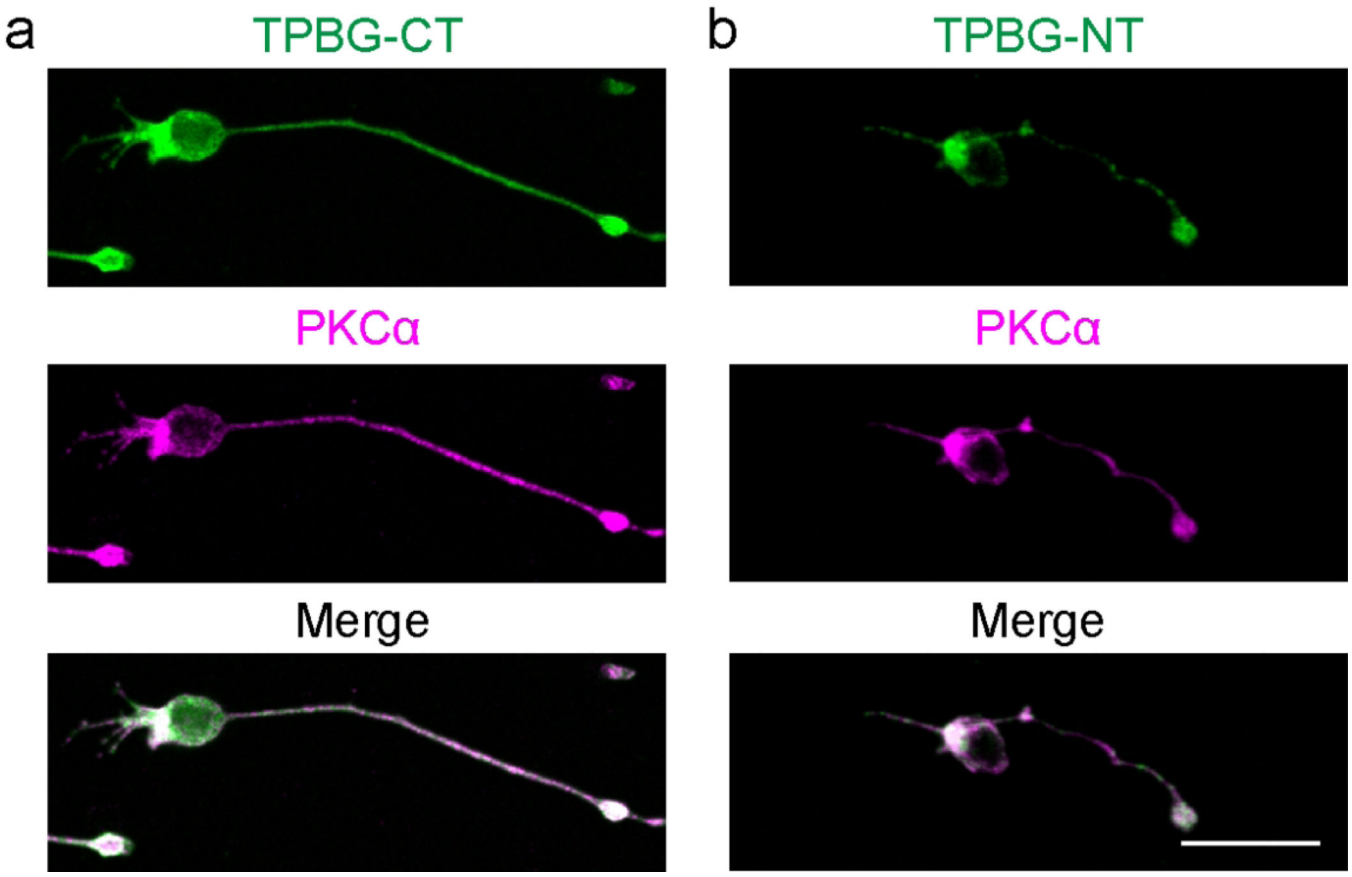

Figure 2: TPBG is expressed in rod bipolar cells.

Confocal microscopy of dissociated wild type RBCs labeled with anti-TPBG-CT (green; a) or anti-TPBG-NT (green; b). Anti-PKCα (magenta) was used to identify RBCs. Sites of co-localization appear white. Z-projections of 3 sections were used with a Z-step distance of 0.297 μm. Scale bar: 20 μm.

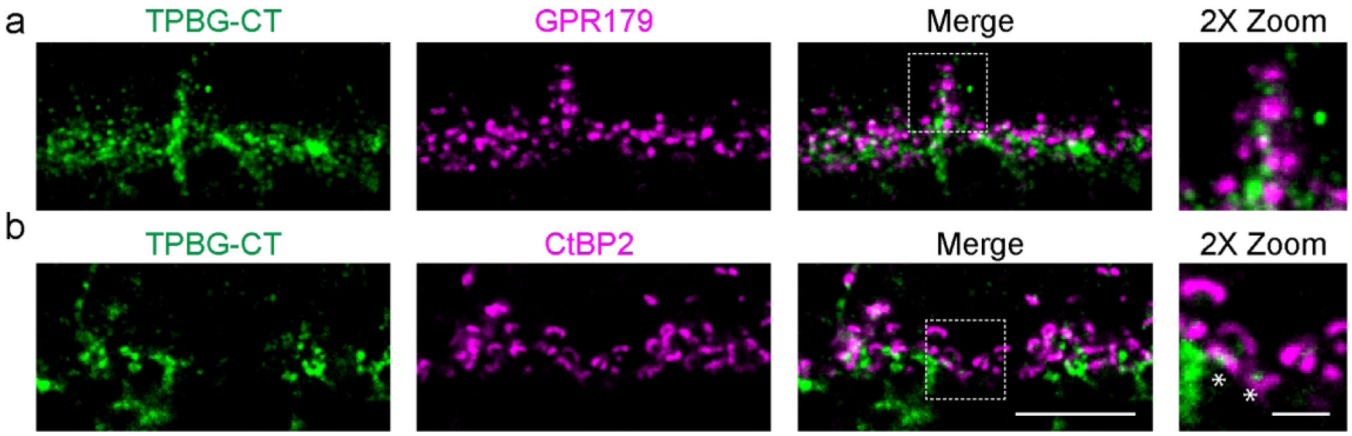

Figure 3: TPBG is present in distal RBC dendrites.

Confocal microscopy of wild type retina sections labeled for TPBG (green) and GPR179 (magenta; a) or CtBP2 (magenta; b). 2X zoom of boxed regions (right panels). Asterisks mark TPBG-positive puncta within CtBP2-positive synaptic ribbons. Sites of co-localization appear white. Z-projections of 3 sections were used with a Z-step distance of 0.297 μm. Scale bars: 10 μm (main panels); 2.5 μm (zoomed panels).

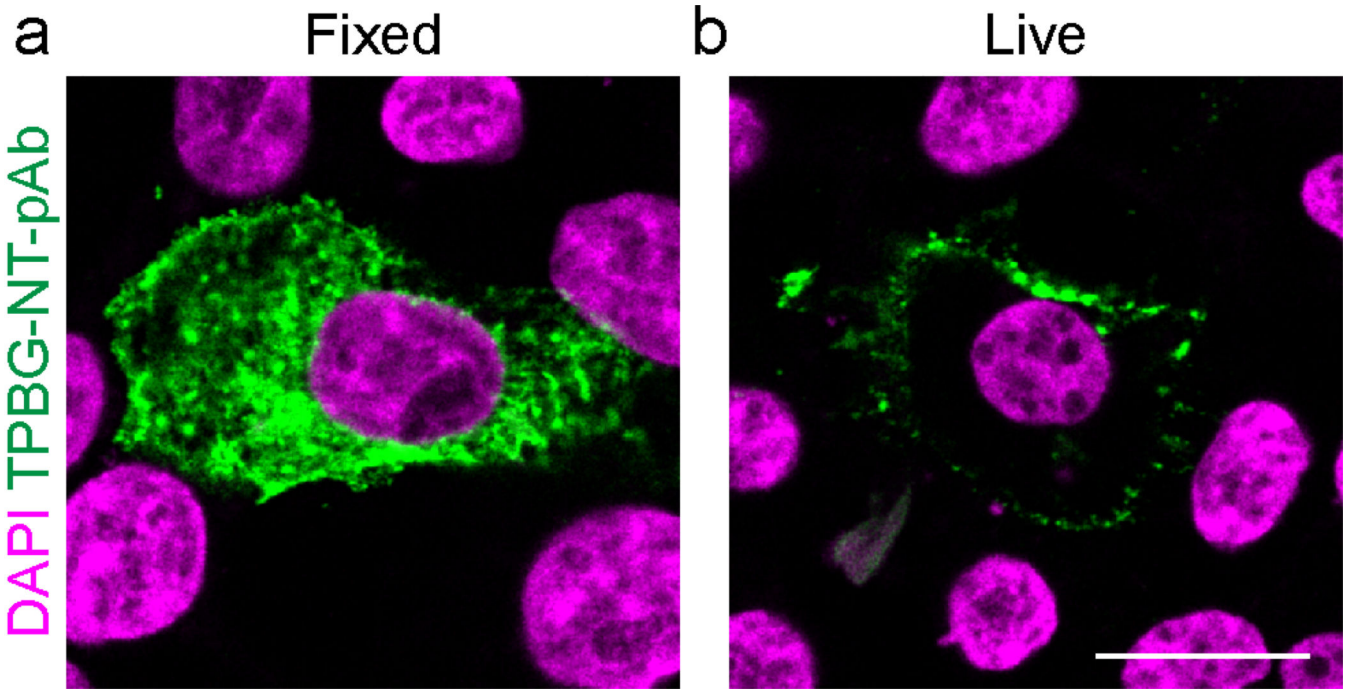

Figure 4: TPBG is localized to the plasma membrane in transfected HEK293 cells.

Confocal microscopy of (a) fixed and permeabilized and (b) live HEK293 cells transfected with cDNA corresponding to full-length mouse TPBG and labeled with an antibody against the extracellular domain of TPBG (anti-TPBG-NT-pAb). The nuclear stain DAPI (magenta) was used to label cell nuclei. Scale bars: 20 μm.

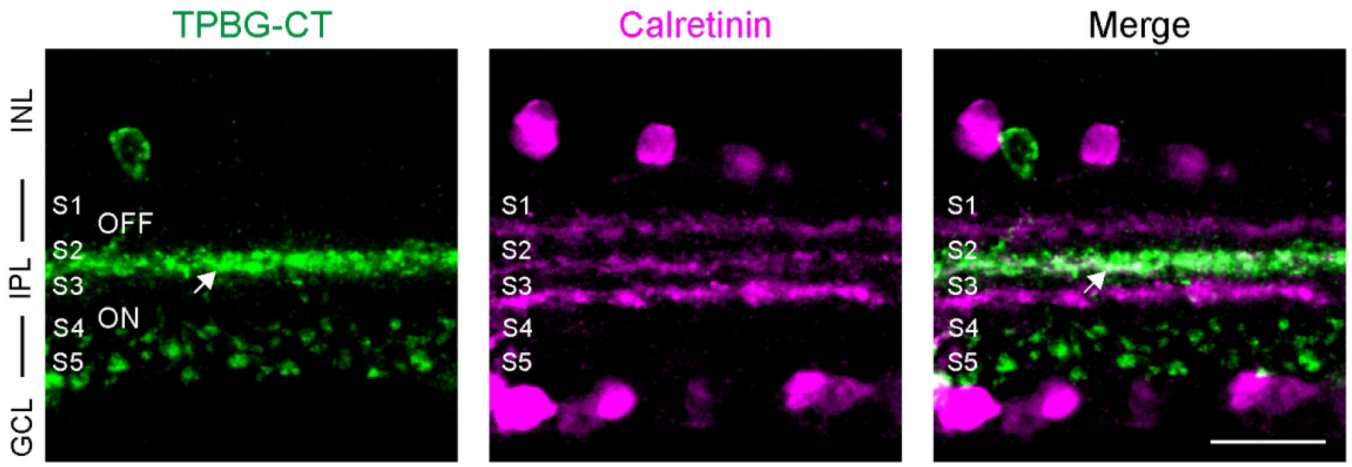

Figure 5: TPBG is present in sublamina 2/3 of the IPL.

Confocal microscopy of wild type adult retina sections labeled for TPBG-CT (green) and calretinin (magenta). Layers were determined by DAPI nuclear staining (not shown), and sublamina were labeled based on calretinin staining. Z-projections of 5 sections were used with a Z-step distance of 0.415 μm. INL: inner nuclear layer; IPL: inner plexiform layer; GCL: ganglion cell layer. Scale bar: 10 μm.

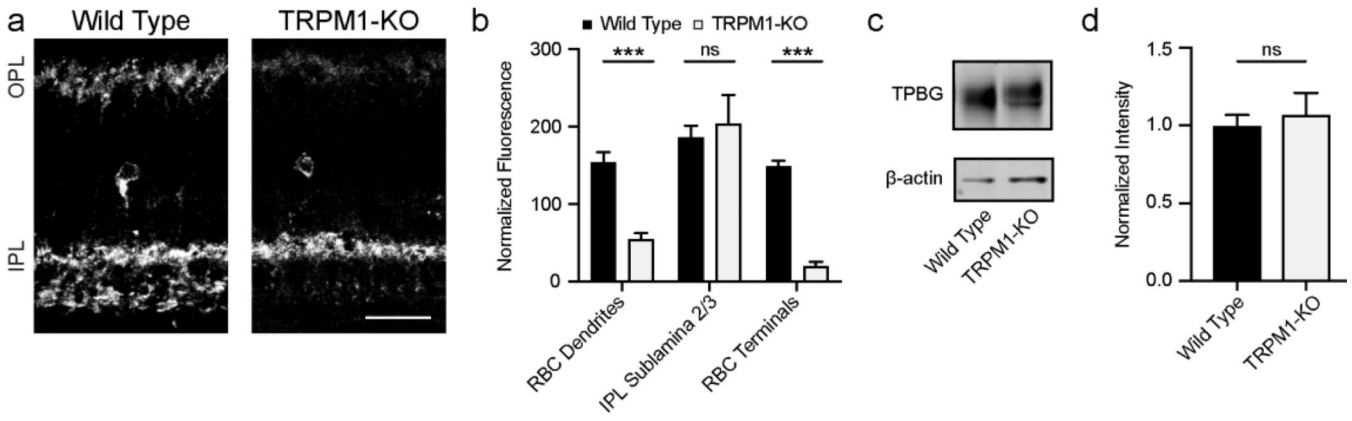

Figure 6: TPBG immunofluorescence is reduced in TRPM1-KO retinas.

(a) Characteristic confocal microscopy of retina sections from wild type and TRPM1 knockout (TRPM1-KO) mice labeled for TPBG-CT. Z-projections of 10 sections were used with a Z-step distance of 0.297 μm. (b) Quantification (mean+SEM) of TPBG fluorescence from different retinal layers normalized to the background fluorescence in the ONL (student's t-tests; RBC dendrites: $p<0.001$; IPL sublamina 2/3: $p=0.66$; RBC synaptic terminals: $p<0.001$). (c) Characteristic immunoblot using anti-TPBG-CT and β-actin, and (d) quantification (mean+SEM) of TPBG band intensity (~72 kDa) normalized to β-actin (42 kDa) and then to the wild type condition (student's t-test: $p=0.71$). N=4 animals for both immunofluorescence and immunoblot analyses. Scale bar: 20 μm.

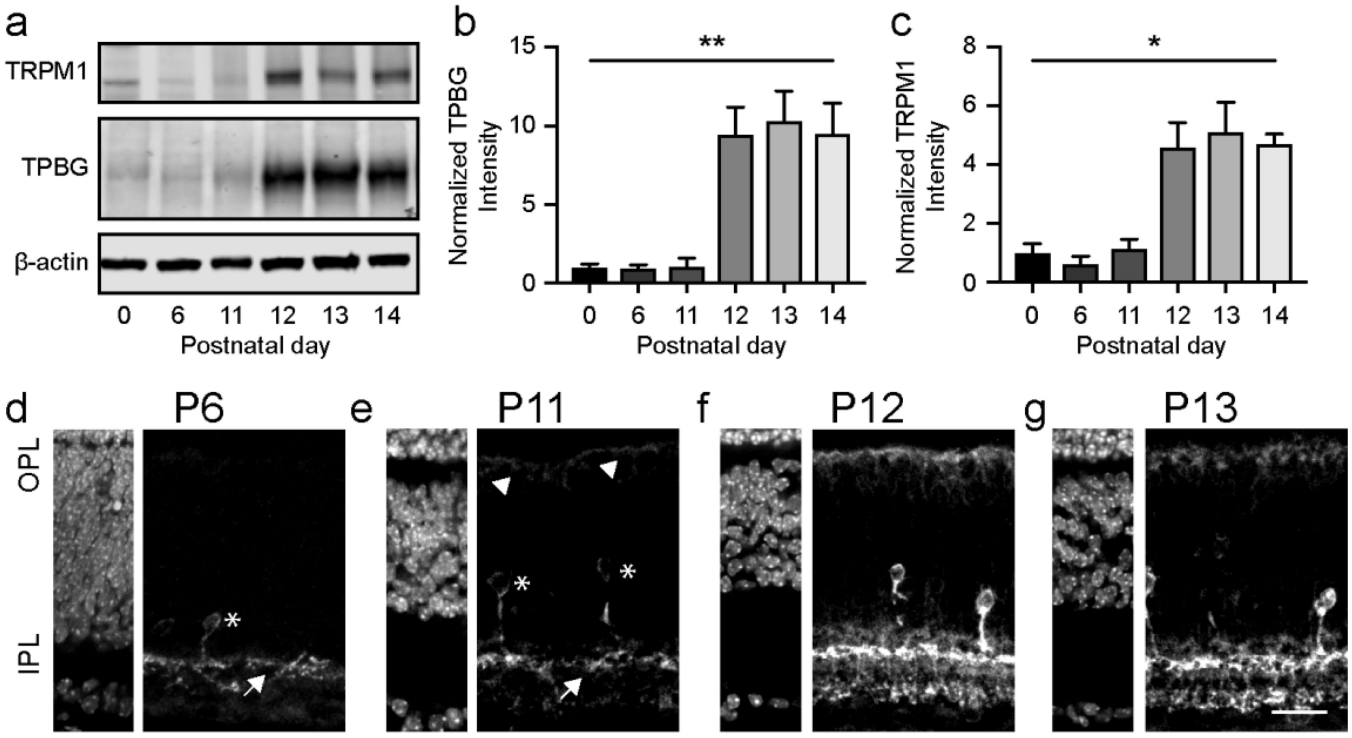

Figure 7: TPBG expression in the retina increases the day before eye opening.

(a) Immunoblot of wild type retinal lysates prepared at different developmental time-points from the same litter and probed for TPBG-CT, TRPM1, and β-actin. Quantification (mean +SEM) of (b) TPBG-CT (one-way ANOVA: $F(5.00, 6.113)=12.35$, $p=0.0038$) and (c) TRPM1 (one-way ANOVA: $F(5.00, 2.778)=12.95$, $p=0.037$) immunoblot band intensity normalized to β-actin and then to the P0 timepoint. Confocal immunofluorescence microscopy of wild type mouse retina sections extracted at P6 (d), P11 (e), P12 (f), and P13 (g) and labeled with DAPI (left panels) or for TPBG-CT (right panels). Asterisks mark TPBG-positive cell bodies in the INL, arrows point to processes in the middle of the IPL, and arrowheads point to RBC dendrites in the OPL. Eye opening occurred between P12 and P13. Z-projections of 7 sections were used with a Z-step distance of 1 μm. N=3 litters of at least 6 mice each for both immunofluorescence and immunoblot analyses. Scale bar: 20 μm.